J2.9 Infrared Imagery Applied for Insights into Wildland Fire Dynamics

Janice L. Coen
National Center for Atmospheric Research, Boulder, CO

1. INTRODUCTION

Crown fire spread rates can vary widely (0-3.1 m s^{-1}, faster in mountainous terrain or when environmental winds are strong) (Rothermel, 1991) and 0.131 – 0.455 m s^{-1} on flat ground with ambient winds ranging from 10-16 km hr^{-1} (Albini and Stocks, 1986), and they can spread several times faster than surface fires (Rothermel 1983, 1991). They can produce copious spotting (that is, where burning embers are lofted ahead of the fire to ignite new fires) leading to control problems at natural and man-made fuel breaks, and predictability is difficult because such fires often affect their atmospheric environment, behaving erratically and sometimes dangerously (National Wildfire Coordinating Group, 1994).

A good physical understanding of crown fire dynamics requires a clear picture of the 3-dimensional winds in and near the fire, including the flaming combustion zone and the convective motions produced by the fire. The mechanisms for their extreme behavior and rapid spread are not well understood, in part because detailed observations are rare - most remote sensing instruments cannot capture the very small temporal and spatial scales in the convective processes that determine fire spread. These observations and analyses present a unique high spatial and temporal resolution perspective into the motions within a naturally evolving crown fire, viewed in profile, propagating up a forested 20° slope under light environmental winds of 3 m s^{-1} during the FROSTFIRE experiment in interior Alaska. Our purposes are to calculate combustion zone winds and fire spread rates, derive statistics summarizing fire winds, and use these to study the mechanisms for the rapid propagation of crown fires.

2. FIELD EXPERIMENT DESCRIPTION

FROSTFIRE was a landscape-scale research project conducted in the boreal forest of interior Alaska that focused on the long-term ecological effects of fire. The setting was the Caribou - Poker Creeks Research Watershed (CPCRW) Long-Term Ecological Research site, a 104 km^2 basin approximately 40 km northeast of Fairbanks, near the town of Chatanika, Alaska (latitude: 147° 30‘ W, longitude: 65° 10’ N). Within the 1050-hectare perimeter, during the experiment, prescribed fires mimicking natural conditions burned 430 ha of mostly black spruce, leaving the hardwoods standing. The major burning occurred over 3 days (8-10 July 1999) while within the window of prescribed burning conditions, followed by several days of smoldering. For more details, see Hinzman et al. (2003)

Terrain. CPCRW is part of a large area of rolling forested hills covered by boreal forest. Ridge elevations range from 450-900 m with rises of 150-500 m above the adjacent valleys. The topography in the area of the FROSTFIRE burn is shown in Fig. 2. The dominant terrain features within the prescribed burn perimeter are Caribou Peak (773 m MSL) and Helmer’s Ridge (630 m MSL).

Fuel/Vegetation. CPCRW is a permafrost-dominated watershed. Three primary vegetation types characterized watershed. The first was closed and open coniferous forests of black spruce. This highly flammable vegetation is the climax vegetation type on north slopes in the research area. They grow tall and thin, rarely exceeding 15 m in height or 0.25 m in diameter, while half the trees in a stand may be less than 0.05 m in diameter. Based upon photos of the burn area, the treetops in the data field of view were approximately 10 m above ground, and spaced closely together with stems often only a couple meters apart. Fire spread freely throughout the black spruce in this experiment. The remainder of the site was dominated by closed hardwood forests of paper birch and quaking aspen on south-facing slopes, boggy sphagnum-dominated wetlands along the stream, and caribou moss on exposed ground. Dwarf tree scrub and tall scrub occur in the valley bottom and on some ridgelines.

Fuel loads given in the FROSTFIRE burn plan (Wilmore et al., 1998) were estimated using an aerial photo series and previously published data from other interior sites (Dymess, Van Cleve, and Levison, 1989). Based on these works, Wilmore et al. (1998) estimate that aerial

Fig. 1. Image of extreme fire behavior (forward burst) obtained during the International Crown Fire Modeling Experiment. (Photo courtesy of the Canadian Forest Service.)

* Corresponding author address: Janice L. Coen, NCAR. P. O. Box 3000, Boulder, CO 80307; email: janicec@ncar.ucar.edu; phone: 303 497-8986; fax: 303 497-8181

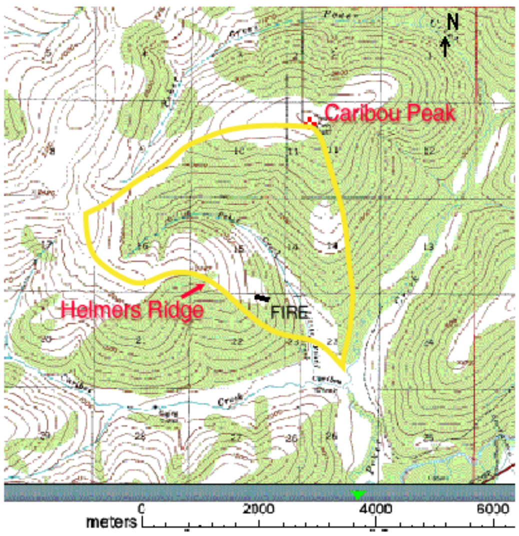

Fig. 2. (a) Terrain with locations of Caribou Peak (imager located approximately 200 m southwest of peak) and general area of the fire. The thick contour shows the FROSTIFIRE burn perimeter. The dark line shows the approximate location of the data cross section within the broader fire area

biomass totaled approximately 5.16 kg m^{-2} and the forest floor totaled 12.3 kg m^{-2} in the black spruce stands. Above ground biomass for the aspen and birch were estimated at 5.60 kg m^{-2}. Forest floor biomass was estimated between 7.85 and 10.8 kg m^{-2} for the birch and aspen stands.

Weather. The weather conditions were recorded at two surface stations at CPCRW during the burn period (not shown). The conditions at midday on 10 July 1999 in the area of the fire were approximately 20-25 °C, about 30% relative humidity, with winds from the northeast at 2-4 m s^{-1}. The flows were upslope as the dark topography began warming in the sun.

Fire. Most of the burning occurred over a 3-day period from 8-10 July 1999, followed by several days of smoldering. The 10 July operational plan called for more firing, and as of 1100 LST, only small fires were smoldering from the previous night's ignitions. However, as the solar heating increased, the northeasterly wind increased, fanning the smoldering fires in the lowest part of the valley, spreading these fires toward the top of Helmer's Ridge (see Fig. 3). Stands of black spruce flared up and the fire spread rapidly upslope in running crown fires. Positioned 2.6-3.2 km across the valley from the fire, we recorded data of several crown fire periods of varying intensity ranging from smoldering fires to running crown fires. Although the fires on this day were originally manually ignited, they evolved as natural fires.

3. INSTRUMENT AND DATA DESCRIPTION

Fig. 3. Fire climbing ridge, viewed from Caribou Peak during this run. East is to the left, west is to the right.

An Inframetrics ThermaCAM PM380, a digital, high-resolution infrared imager. was used to detect high temperature regions produced by incandescent soot particles in and near the flaming combustion region of the fire, and produce a sequence of high frequency (60 per second), high resolution (0.375 x0.8 m) 2-dimensional (x-z) imagery of temperature over a 1-min. sequence, limited by the fire's rapid exit from the image. Although the basic unit had a 17^{o} x 16^{o} field of view, a 4^{o} x 4.2^{o} telephoto lens was added, so at a range of 2800 m, for example, each pixel represented an area of 0.376 x 0.845 m.

By detecting the radiant energy in the 3.4 - 5.0 μm wavelength band, the imager produces data of the radiating object's temperature, creating 2-dimensional color video images of hot, swirling air mixed with products of combustion in the fire, detailing their size, structure, and temperature (Fig 4.)

The gradient-based image flow analysis methods described in detail in Clark et al. (1999) were used to extract fire wind estimates from the temporal and spatial evolution of the temperature field in the image plane.

4. RESULTS

Here we present analysis of data comprising approximately 1 minute of crown fire propagation over the period 13:29:08 – 13:30:07 local time on 10 July 1999. This period short because uninterrupted periods are required for this analysis, and in this sequence, the fire traveled entirely across the field of view and exited, requiring us to re-aim the imager.

Fig. 4 shows a selection of temperature images. The data was taken over a segment of imager range XRG2 corresponding to the temperature range 500-800 C (this color scale is shown to the left of each image, where dark colors represent colder temperatures and the bright colors represent warmer temperatures). The distance to the image is approximately 2.8 km. (The *z*-axis appears compressed due to the de-interlacing of these images where odd and even rows are separated into 2 sequential images spaced $1/60^{th}$ of a second apart.)

The high temperature regions identify the flaming combustion of an envelope of volatile gases released by pyrolyzing surface fuel and individual trees. These gases are not instantly consumed, and pockets may be transported some distance before entrainment with environmental air produces the stoichiometric conditions needed for combustion. Although one must be cautious in interpreting the temperature data, the temperature values in the data are well within the range of temperatures expected for combustion in diffusion flames. Incomplete combustion is concurrently producing products of incomplete combustion (PICs) such as soot. Radiating particles from these processes produce the infrared radiation detected, until they mix and radiatively cool enough to be outside our selected

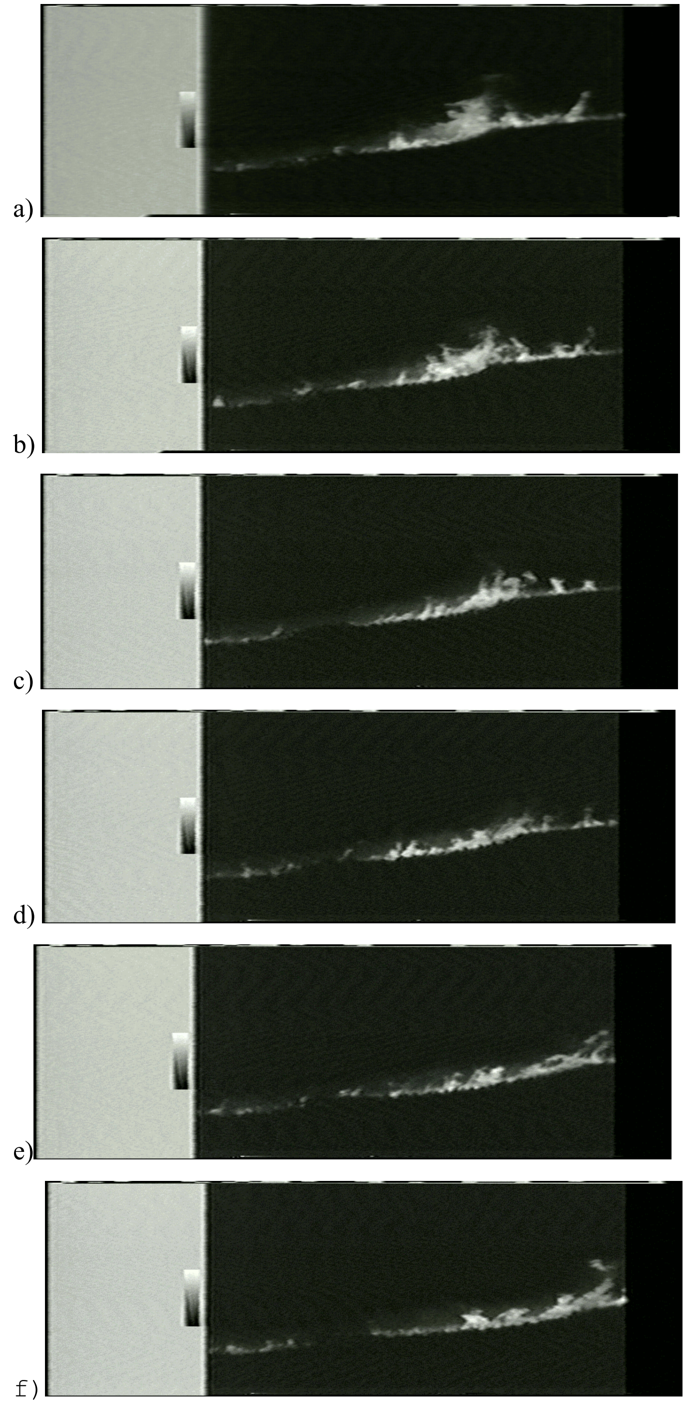

Fig. 4. Sequence of temperature images at times relative to the beginning of the sequence: (a) 0.217 sec, (b) 1.85 sec, (c) 4.00 sec, (d) 9.77 sec, (e) 22.13 sec, (f) 41.37 sec, and (g) 54.00 sec. The times of the images correspond to the times of images in Fig. 6. The grayscale image data correspond to temperatures of the range 500 (black) -800 ^{o}C (white), as shown in the temperature scale to the left of each image. The fire is traveling from left to right. Due to de-interlacing, the vertical scale is compressed – the image area is 195 m x 205 m.

detection temperature range.

At the base of the flaming combustion region (the bright regions), one can discern the (dark, cool) treetop outline, although individual trees are spaced slightly closer than our resolution can show. This outline of treetops (i.e. the highest vertical point at which the temperature is not raised over ambient) was followed over time to identify the ridgeline in the infrared data. This showed the slope was approximately 20 °. This slope is used in later sections to calculate the velocities parallel to the surface.

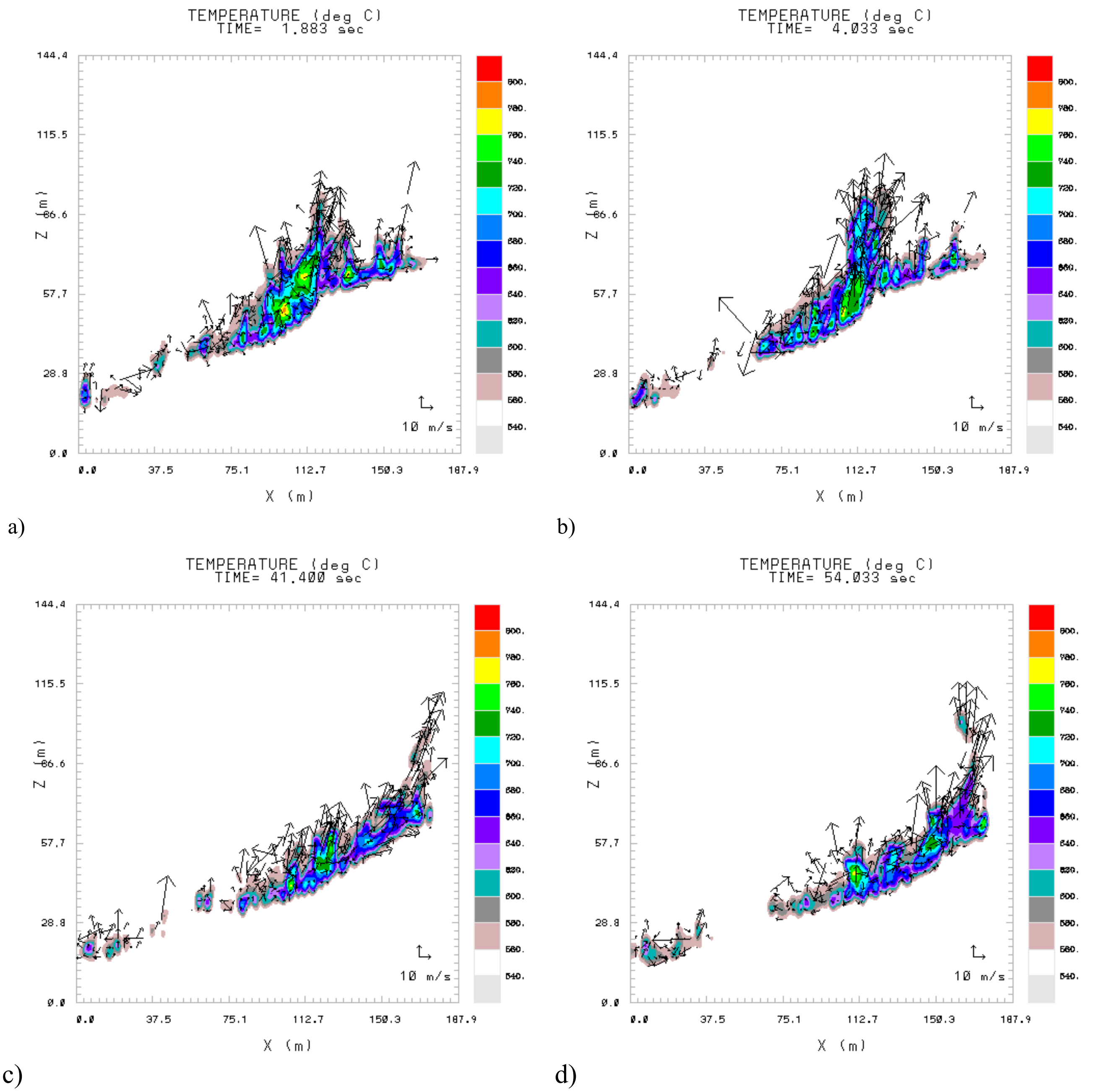

Fig. 5. Sequence of images obtained from image flow analysis (with calculated vectors) during profile sequence. This image corresponds to the dark line in Fig. 2a. (East is to the left.) Colored contours show the temperature detected by the infrared imager (cut off by a 40 °C above ambient threshold). The vectors show the calculated flow velocities. Every 8th point in the *x* direction and every 4th in the *z*-direction are plotted.

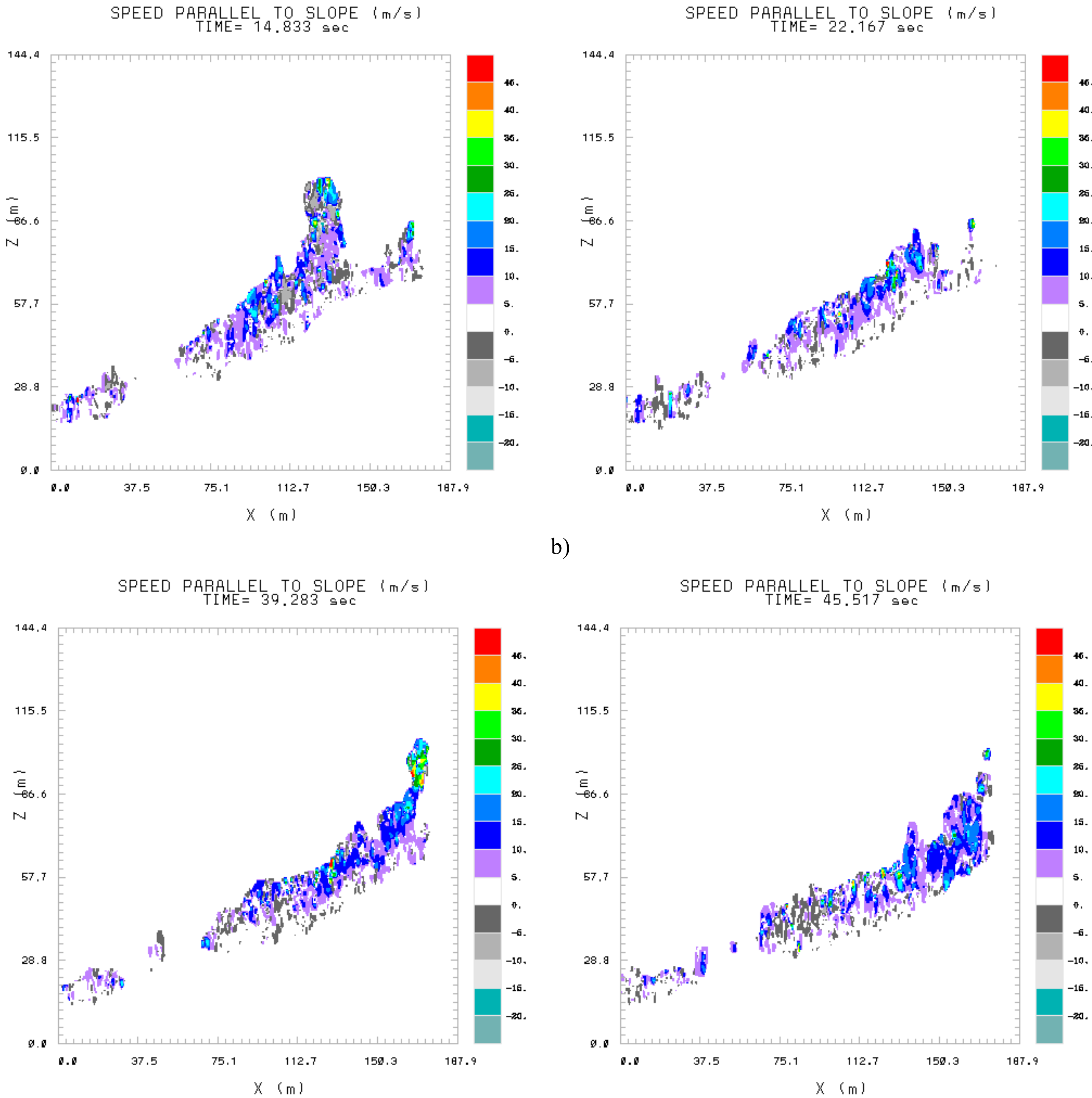

a) b)

d)

Fig. 6. Motions calculated from image flow analysis. The velocity parallel to the slope is shown.

The images themselves show a crown fire traveling upslope from left to right. Some features are apparent. Although the crown fire is pyrolyzing and igniting the gases from individual trees, the convective heat from several trees rapidly loses the scale of individual trees (approximately 1-5 m apart) and agglomerates into many larger-than-individual-tree-scale convective plumes.

Clearly, these elements are very buoyant. However, under an upslope wind (from the left in Fig. 5) that is partially ambient and no doubt modified by the fire itself, the plumes do not simply rise vertically, but travel some distance parallel to the slope before buoyancy forces take over, and the plume rises much more vertically, although tilted in the downwind direction. One consequence is that the spread of the fire up the slope is characterized by a sequence of forward bursts of flame that extend forward along the slope before bending upwards.

Velocities. The air velocities calculated using the image flow analysis, superimposed upon the temperature field, are shown at several times during this sequence in Fig. 5. These velocities in and near the fire cannot be regarded as an external force directing the fire, but are themselves partly driven by the fire, and are an intrinsic part of the dynamics of fire propagation

Velocities parallel to the slope. A more physically relevant estimate of wind speeds along the surface than the horizontal wind component is the component of the wind along the slope. This was obtained by calculating the dot product of the total wind vector with the gradient slope, where the surface is approximated to rise to the right at 20^{o}. Although the strongest atmospheric winds overall are located in the rising convective plume several tens of meters above the ground, Fig. 6 shows how close the forward bursts described earlier are to the ground. In this 60-second sequence, velocity components parallel to the surface of 10 m s^{-1} are routine, with frequent bursts of 25 m s^{-1}. Peak surges of 30 m $s^{-1}$are detectable less than 15 m above the base of the detectable fire. Thus, the speed the explosive fingers travel parallel to the slope is an order of magnitude larger than ambient winds measured by nearby surface weather stations and far more complex than tilting of a buoyant updraft

Using conservative statistical techniques (Fig. 7), we found maximum updrafts of 32-60 m s^{-1}, maximum downdrafts of 18 – 30 m s^{-1}, maximum horizontal wind speeds of 12-28 m s^{-1} representing strong inflow into the base of the convective updrafts (apparently recirculating air and incomplete combustion products from the fire), and maximum winds parallel to the slope of 28-48 m s^{-1}. Average spread rates for a flank of the fire were 0.75 – 1.11 m s^{-1}, with a peak spread rate over any 10 s period of 1.26 m s^{-1}. These extreme winds and rapid spread rates could not be attributed to the weak environmental upslope winds of 3 m s^{-1}. These upslope bursts of flame initially have a strong along-ground component that in this situation exceed ambient environmental winds (the winds generally considered to be 'driving' the fire) by a factor of 10. These bursts play an active role in propagating the crown fire and point towards a powerful, dynamic, mechanism of fire spread at the heart of anecdotes where firefighters report being overtaken by 'fireballs'.

Spread Rates. It is difficult to calculate an overall canopy spread rate for this fire. This is because, rather than a smoothly spreading interface, what we observed were repeated flame-filled bursts from the fire's core upslope along the treetop. These ignited patches of treetop ahead of the main fire flared up in intensity as the most dynamically active core of the fire approached. However, our perspective did allow us to calculate the spread rate in the leading edge right flank of the fire, which was oriented towards our imager and surged toward the right of the imagery during this period. During the first 50 sec of this sequence, this front traveled 43 m upslope, giving an average spread rate of 0.75 m s^{-1} for this feature. This was not steady – the second half of this period was more active, making 75% of its move during the period 25.5 sec – 50.5 sec, where the spread rate over this period is calculated to be 1.11 m s^{-1} (2.48 mph). The maximum over any 10-second period was calculated to be 1.26 m s^{-1} (2.82 mph). While crown fires have been estimated to travel at a wide range of speeds, the spread rates calculated in this work are substantial, especially considering that the environmental winds were comparatively light.

5. DISCUSSION

The picture that emerged was dynamically complex and defied the common notion of one large convective plume or many tree-scale plumes rising separately, simply accelerating under the force of buoyancy. Instead, repeated upslope surges of convective plumes represented a scale larger than individual trees. These explosive surges initially had a strong along-ground component that played an active role in propagating the crown fire (lying low enough to both ignite and preheat/dry canopy fuel ahead of the fire) and points towards a powerful, dynamic mechanism of fire spread.

These observations and analyses present a unique high spatial and temporal resolution perspective into the motions within a crown fire propagating up a forested slope in interior Alaska.

The mechanism for rapid crown fire spread has been attributed (Rothermel, 1991) to either strong environmental winds (in the case of so-called "wind-driven fires"), to momentum feedback from the vertical updraft to increase surface turbulence in the surface winds resulting in increased radiational heating of surface fuels, or to downbursts of wind from convective cells. None of these explanations is satisfactory here, as the ambient flow is only 3 m s^{-1}, even though bursts of 20-25 m s^{-1} were detected within 20 m of the ground (we cannot detect motions very near the surface, because it is obscured and the pixel temperature is diluted by trees). Also, the inflow to these extremely strong updrafts over a very narrow depth appears very organized and smooth, showing none of the signs of turbulent dissipation. And, no clouds were present to produce downdrafts. Clearly, the source of the momentum must be the buoyancy produced by the fire, but these bursts, although turbulent in nature, are coherent features.

Our perspective and subsequent analysis of extreme fire behavior adds to the observations of Radke et al. (2000), which first recognized these sudden flame-filled fingers and theorized that they were traveling near enough the ground to ignite the fuel. These fingers are present throughout our data as well, although our view of fires in profile allows us to refine their interpretations.

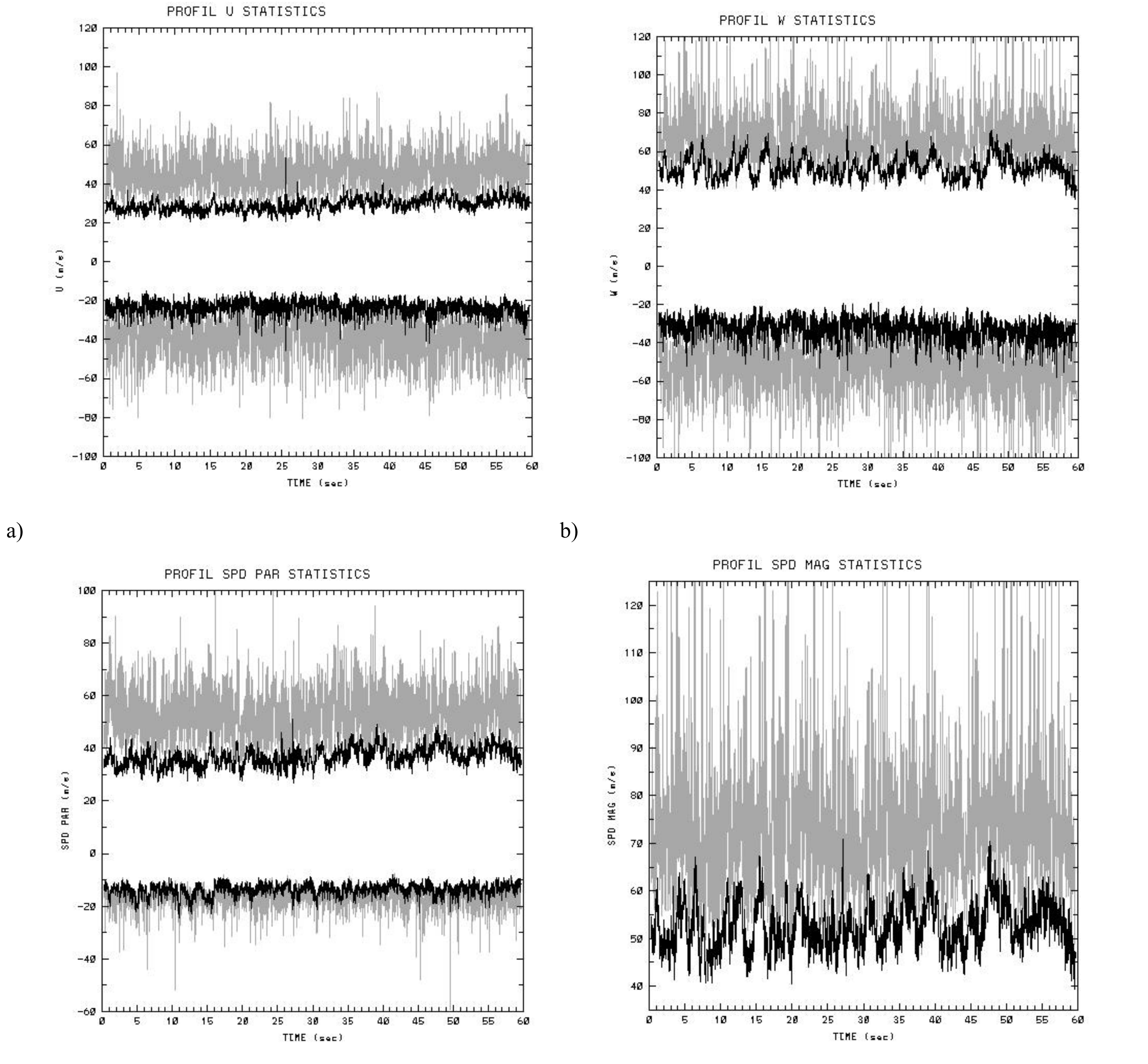

Figure 7. Velocity statistics for domain-wide maximum and minimum: a) *u* (horizontal) velocity component, b) *w* (vertical velocity) component, c) extrema for the (derived) velocity component parallel to the slope, d) the maximum air speed. Actual calculated maximum values are shown in gray, while black lines show expected extrema that are +/- 5 standard deviations from the image-wide mean statistical values.

The overall picture that emerges from these results is dynamically complex and defies the common notion of one large convective plume or many tree-scale plumes that rise separately, simply accelerating under the force of buoyancy. Instead, the picture that emerges is a sequence of surges composed of many interacting convective plumes that represent a scale larger than individual trees. These explosive upslope bursts of flame initially have a strong along-ground component that in this situation exceed ambient environmental winds (the winds generally considered to be ‘driving’ the fire) by a factor of 10. These bursts play an active role in propagating the crown fire and point towards a powerful, dynamic, mechanism of fire and could explain the ‘fireballs’ or bursts of hot air (and flame) documented by firefighters overrun by crown fires.

6. REFERENCES

Albini, F. A., and B. J. Stocks, 1986: Predicted and observed rates of spread of crown fires in immature Jack pine. Combust. Sci. and Tech., **48**, 65-76.

Clark T. L., L. F. Radke, J. L. Coen, and D. Middleton, 1999: Analysis of Small-Scale Convective Dynamics in a Crown Fire Using Infrared Video Camera Imagery. J. Appl. Meteor., **38**, 1401-1420.

Dymess, C. T., T. K. Van Cleve, and J. D. Levison, 1989: The effect of wildfire on soil chemistry in four forest types in interior Alaska. Canadian J. of Forest Research, **19**,1389-1396.

Hinzman, L. D., M. Fukuda, D. V. Sandberg, F. S. Chapin III, and D. Dash, 2003: FROSTFIRE: An experimental approach to predicting the climate feedbacks from the changing boreal fire regime. J. Geophys. Res., **108**, 8153-8158.

National Wildfire Coordinating Group, 1994: Introduction to Wildland Fire Behavior S-190. National Interagency Fire Center, Boise. NFES #180. 66 pp.

Radke, L. R., T.L. Clark, J. L. Coen, C. Walther, R. N. Lockwood, P.J. Riggin, J. Brass, and R. Higgins, 2000: The Wildfire Experiment (WiFE): Observations with airborne remote sensors. Canadian J. Remote Sensing, **26**, 406-417.

Rothermel, R. C., 1983: How to predict the spread and intensity of forest and range fires. Gen. Tech. Rep. INT-143. Ogden, UT: U.S. Dept. of Agriculture, Forest Service, Intermountain Research Station. 161 pp.

Rothermel, R. C., 1991: Predicting behavior and size of crown fires in the northern Rocky Mountains. Res. Pap. INT-438. Ogden, UT: U.S. Dept. of Agriculture, Forest Service, Intermountain Research Station. 46 pp.

Wilmore, R., K. Slaughter, M. Theisen, and J. Roessler, 1998: FROSTFIRE Research Prescribed Burn Plan. BLM Alaska Fire Service, 62 pp.